Journal of Pharmacy

ORIGINAL ARTICLE Open Access

Green-synthesized silver nanoparticles from *Anisophyllea corneri* leaf extract and its antimicrobial and cytotoxic activities

Ika Rizky Fadhillah[1], Muhammad Taher[2,3*], Mokhamad Nur[1] & Deny Susanti[4]

ABSTRACT

Introduction: The escalating global threat of multidrug-resistant pathogens necessitates innovative approaches to combat drug resistance. Silver nanoparticles (AgNPs) have emerged as promising candidates due to their potent antimicrobial and anti-cancer properties. Green synthesis of AgNPs using plant extracts offers an eco-friendly and cost-effective method. This study focuses on the green synthesis of silver nanoparticles (AC-AgNPs) using *Anisophyllea corneri* leaf extracts and evaluates their antimicrobial and cytotoxic activities.

Materials and methods: An eco-friendly synthesis approach was employed, utilizing *A. corneri* leaf extracts as reducing agents. Liquid Chromatography-Mass Spectrometry (LC-MS) was utilized for phytochemical profiling. The synthesis process was optimized at various temperatures (60ºC, 70ºC, 80ºC) and pH levels (4, 9) to achieve optimal AgNPs outcomes. Characterization of AC-AgNPs included UV-Vis spectrophotometry, FTIR, SEM, Zeta potential, and Particle Size Analyzer (PSA). Antimicrobial evaluation was conducted against four bacteria (*Pseudomonas aeruginosa*, *Escherichia coli*, *Bacillus subtilis*, *Staphylococcus aureus*) using paper disc diffusion. Cytotoxicity was assessed through the MTT assay on MCF-7 (breast cancer cell line).

Results: *A. corneri* leaf extract exhibited abundant active compounds facilitating the reduction of silver ions. Optimization revealed that 70ºC at pH 9 produced AC-AgNPs with a minimal particle size of 135.5 nm and a stable zeta potential (-45.1±11.7 mV). AC-AgNPs displayed a spherical morphology. Antimicrobial trials demonstrated moderate efficacy against the tested bacteria, with inhibition zones ranging from 8 to 10 mm. Additionally, AC-AgNPs exhibited cytotoxic potential with a moderate IC_{50} of 74.9 µg/mL.

Conclusion: The green synthesis, characterisation and biological activities of AgNPs from *A. corneri* leaf extracts have been established. It is recommended to optimise the synthesis process and validate the biological activities.

ARTICLE HISTORY:

Received: 1 December 2023
Accepted: 29 January 2024
Published: 31 January 2024

KEYWORDS:

Anisophyllea corneri, antimicrobial, cytotoxic, green synthesis, silver nanoparticle

HOW TO CITE THIS ARTICLE:

Fadhillah, I. R., Taher, M., Nur, M. and Susanti, D. (2024). Green-synthesized silver nanoparticles from *Anisophyllea corneri* leaf extract and its antimicrobial and cytotoxic activities. *Journal of Pharmacy,* 4(1), 103-115.

doi: 10.31436/jop.v4i1.265

***Corresponding author:**
Muhammad Taher
Email: mtaher@iium.edu.my

Authors' Affiliation:

[1]*Department of Food Science and Biotechnology, Faculty of Agricultural Technology, Brawijaya University, Malang, Indonesia*
[2]*Department of Pharmaceutical Technology, Kulliyyah of Pharmacy, International Islamic University Malaysia, Kuantan*
[3]*Pharmaceutics and Translational Research Group, Kulliyyah of Pharmacy, International Islamic University Malaysia, Kuantan, Pahang, Malaysia*
[4]*Department of Chemistry, Kulliyyah of Science, International Islamic University Malaysia, Kuantan, Pahang, Malaysia.*

Introduction

The rise of multidrug-resistant pathogens has significantly contributed to the surge in infectious diseases, becoming a leading cause of global mortality (WHO, 2023; Tanwar et al., 2014). The extensive use of antibiotics has been a primary driver of bacterial resistance, leading to severe consequences such as increased mortality, prolonged hospitalization, and substantial economic losses (O'Bryan et al., 2018; Patel et al., 2008). To address this critical issue, innovative strategies to combat drug resistance effectively are required.

Nanotechnology has emerged as a promising solution to tackle drug resistance, with silver nanoparticles (AgNPs) gaining considerable attention for their potent antimicrobial properties. Various studies have highlighted the efficacy of AgNPs against drug-resistant bacteria, including *Escherichia coli*, *Klebsiella pneumoniae*, *Salmonella typhimurium*, and *Salmonella enteritidis*, showcasing their potential to inhibit microorganisms (Loo et al., 2018). Additionally, AgNPs have demonstrated high cytotoxicity against cancer cells such as MCF-7 and Caco-2 (Shelembe et al., 2022; Böhmert et al., 2012).

Despite their therapeutic potential, conventional methods for AgNP synthesis involve the use of hazardous chemicals, posing risks to human health and the environment. In response to these challenges, researchers have shifted towards green synthesis approaches, utilizing natural extracts to produce AgNPs. Green synthesis offers environmental friendliness by eliminating the need for harmful chemicals (Zhang et al., 2016). In this context, *A. corneri*, a plant rich in active compounds and known for its antimicrobial potential, presents an opportunity for green AgNP synthesis (Bari et al., 2021; Onivogui et al., 2016).

This study aims to employ *A. corneri* leaf extract for the green synthesis of AgNPs and investigate their antimicrobial and cytotoxic activities. Antimicrobial efficacy will be assessed against four bacterial strains (*Bacillus subtilis*, *Staphylococcus aureus*, *Pseudomonas aeruginosa*, and *Escherichia coli*) using the disc diffusion method. Cytotoxicity will be evaluated on the breast cancer cell line (MCF-7) through the MTT assay. Additionally, the active compounds present will be analysed using Liquid Chromatography-Mass Spectrometry (LC-MS).

Materials and methods

Plant Sample Collection and Extraction

Fresh leaves of *A. corneri* (voucher specimen PIIUM0317) were collected and deposited at the Herbarium Kulliyyah of Pharmacy, International Islamic University Malaysia Kuantan Campus, Kuantan, Malaysia. The leaves underwent air-drying at 40°C, followed by mechanical grinding into a fine powder. A total of 50 grams of the powdered leaves were mixed with 500 mL of ethanol-water (80:20 v/v, Ethanol 95%, GENE Chemical) in a 500 mL Erlenmeyer flask. Ultrasonic-assisted extraction (UAE) was conducted at 48°C for 40 minutes using a Qsonica Ultrasonic Sonicator Converter Model CL-334. The resulting leaf extract was filtered using NICE Qualitative 102 filter papers and stored at 4°C (Eze et al., 2019).

Liquid Chromatography Mass Spectrometry Quadrupole Time-of-Flight (LC/MS-QTOF) Analysis

The *A. corneri* leaf extract was dried with a rotary evaporator at 130 rpm and 50°C. The dried extract was reconstituted in methanol to a final concentration of 10 mg/ml, then further diluted to 1 mg/ml with methanol. Prior to LC/MS-QTOF analysis (Agilent Technologies, SA, USA), the extract was filtered through a 0.22 µm pore size syringe filter. The LC/MS analysis employed an Agilent ZORBAX Eclipse Plus C18 Rapid Resolution HT (2.1 x 100 mm) 1.8 µm column with a gradient elution program. Mass spectrometry was operated in positive electrospray ionization (ESI) mode. Data analysis was performed using Agilent Mass Hunter Qualitative Analysis B.05.00 software (Agilent Technologies, Santa Clara, CA, USA).

Preparation of Silver Nitrate ($AgNO_3$) Solution

1 mM $AgNO_3$ solution was prepared by dissolving 0.0459 grams of $AgNO_3$ powder (EMSURE, Macedonia) in 270 mL of deionized water.

Green Synthesis of AC-AgNPs

In the green synthesis process, 30 mL of *A. corneri* leaf extract was gradually added to a 270 mL $AgNO_3$ 1 mM solution under continuous stirring (100 rpm) using a magnetic stirrer. The mixture was divided into three equal portions of 100 mL each and stirred and heated at temperatures of 60, 70, and 80°C for 90 minutes. After 90 minutes, each mixture was further divided into two equal portions of 50 mL each. In one portion of each temperature treatment, 1 M NaOH was added drop by drop until reaching pH 9. The synthesized solution was then centrifuged at 11,000 rpm for 30 minutes at 4°C for purification using a Supra 22K centrifuge (Korea). The resulting pellet of AC-AgNPs was resuspended in deionized water and dried at 40°C, stored at room temperature for future use.

Characterization of AC-AgNPs

UV-Vis Spectrophotometer Analysis: AC-AgNPs were sampled at different time points for analysis using a UV-Visible double-beam spectrophotometer (SHIMADZU UV-1800, Japan) in the scanning range of 300-800 nm.

Particle Size and Zeta Potential Analysis: An aqueous solution of AC-AgNPs was analysed using a Malvern Zetasizer instrument at 25°C.

FTIR Analysis: AC-AgNPs powder samples were analysed using a PerkinElmer Dual FT-IR Spectrometer, covering the 400–4000 cm^{-1} range.

SEM Analysis: Images of AC-AgNPs were captured using a Zeiss EVO-50X Scanning Electron Microscopy (SEM) instrument.

Antimicrobial Assay

Four bacterial strains, including two Gram-positive (*Bacillus subtilis* and *Staphylococcus aureus*) and two Gram-negative (*Escherichia coli* and *Pseudomonas aeruginosa*) bacteria, were cultured in nutrient broth medium. Subsequently, they were incubated for 18 hours at 37±1°C. The antimicrobial activity of AC-AgNPs was evaluated using a disc diffusion assay. The cultivated microbes were sub-cultured on Petri dishes, and 10 µL of AC-AgNPs, *A. corneri* plant extract, $AgNO_3$ solutions, and 10% DMSO (negative control) were applied to sterile discs. Amoxicillin discs were used as the positive control. Following this, the Petri dishes were placed in a CO_2 incubator (Binder) at 37°C for 24 hours. The diameter of the inhibition zones around the discs was measured in millimeters and compared with the negative control.

Cytotoxic Activity

Human epithelial breast adenocarcinoma cells (MCF-7) were cultured at 37°C in a 5% CO_2 incubator (Thermo Scientific Heraeus BB15) in Eagle's minimal essential medium (EMEM) (ATCC 30-2003, Manassas, VA) supplemented with 10% fetal bovine serum (FBS) (Gibco, Brazil) and 1% (v/v) penicillin-streptomycin (Nacalai Tesque, INC., Kyoto, Japan). Once the cells reached 80% confluence, they were detached and subcultured. Subsequently, the cells were seeded into a 96-well plate at a density of 15,000 cells per well. Cell Viability Assay: The cytotoxic activity of the synthesized AgNPs was assessed using the 3-[4,5-dimethylthiazol-2-yl]-2,5-diphenyltetrazolium bromide (MTT) colorimetric assay. The seeded cells were exposed to various concentrations of AC-AgNPs (90 µg/mL, 45 µg/mL, 22.5 µg/mL, 11.25 µg/mL, 5.63 µg/mL, and 2.81 µg/mL), $AgNO_3$, and an anticancer drug, Tamoxifen, as a positive control. The cells were incubated for 24 hours. Afterwards, 10 µL of MTT (0.5 mg/mL) was added, and the cells were re-incubated for 4 hours at 37°C. Formazan crystals that formed were dissolved using 100 µL of DMSO (EMPLURA, USA), and they were further incubated for an additional 30 minutes at 37°C. Using a microplate reader, absorbance at 570 nm was measured to determine differences in color intensity.

Results and Discussion

LC/MS-QTOF analysis of A. corneri leaves extract

Initial compound identification was conducted through LC/MS-QTOF analysis by comparing the m/z spectrum of each compound with the METLIN mass spectrum database (Figure 1).

Table 1 provides detailed information on the chemical composition of 55 identified compounds, including their names, molecular formulas, m/z values, masses, and classifications. These compounds belong to various categories such as flavonoids, fatty acyls, tannins, and others. Notably, it is worth noting that some compounds remain unidentified as their data is not available in the METLIN database.

Numerous studies have highlighted the role of various phytochemicals, such as phenolic acids, flavonoids, alkaloids, terpenoids, amino acids, alcoholic compounds, glutathiones, polysaccharides, antioxidants, and organic acids (including ascorbic, oxalic, malic, tartaric, and protocatechuic acid), as well as quinones. These compounds are known for their ability to serve as reducing, capping, and stabilizing agents in the synthesis of AgNPs (Mustapha et al., 2022; Suriyakala et al., 2022; Zuhrotun et al., 2023). Given the observed biological activity of *A. corneri*, it appears to be a promising candidate for the synthesis of AC-AgNPs.

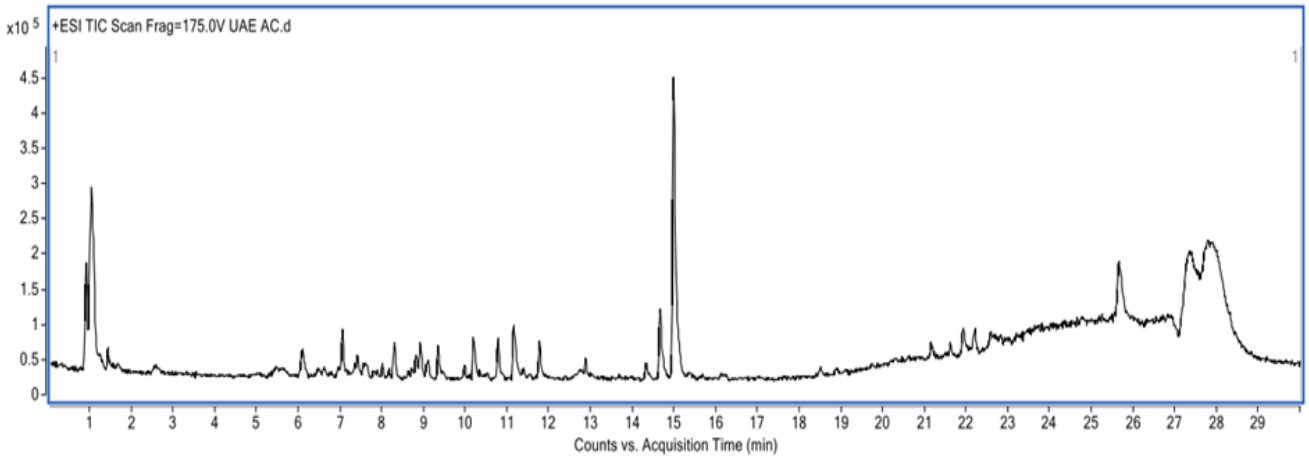

Figure 1: LC/MS Q-TOF Total Ion Chromatogram (TIC) of *A. corneri* Extract

Table 1: Compounds Predicted in *A. corneri* Leaf Extract

Retention time (min)	(M-H)- m/z	Mass	Predicted compound	Predicted molecular formula	Class
1.007	203.0535	180.0644	Paraxanthine	$C_7 H_8 N_4 O_2$	Imidazopyrimidines
1.012	282.0878	562.1613	Physalin H	$C_{28} H_{31} ClO10$	Benzene and substituted derivatives
1.02	385.0923	384.0851	5,6-Dimethoxysterigmatocystin	$C_{20} H_{16} O8$	Sterigmatocystins
1.03	381.0806	358.0916	N1-(5-Phospho-a-D-ribosyl)-5,6-dimethylbenzimidazole	$C_{14} H_{19} N_2 O_7 P$	Benzimidazole ribonucleosides and ribonucleotides
1.031	365.1058	342.117	D-(+)-Cellobiose	$C_{12} H_{22} O_{11}$	Fatty Acyls
1.045	118.0867	117.0794	Isoamyl nitrite	$C_5 H_{11} N O_2$	Organonitrogen compounds
1.047	163.0597	162.0524	3-Hydroxy-3-methyl-glutaric acid	$C_6 H_{10} O_5$	Organooxygen compounds
1.054	295.095	256.1313	2-[4-(3-Hydroxypropyl)-2-methoxyphenoxy]-1,3-propanediol	$C_{13} H_{20} O_5$	Phenol ethers
1.06	236.1498	218.1159	3-hydroxy-sebacic acid	$C_{10} H_{18} O_5$	Hydroxy acids and derivatives
1.57	132.1015	131.0943	N,N-Diethylglycine	$C_6 H_{13} N O_2$	Carboxylic acids and derivatives
2.576	166.0862	165.0788	Gentiatibetine	$C_9 H_{11} N O_2$	Pyranopyridines
5.016	205.0963	187.0625	Deethylatrazine	$C_6 H_{10} Cl N_5$	Triazines
5.453	802.1075	784.0736	Pedunculagin	$C_{34} H_{24} O_{22}$	Tannins
5.531	970.1136	952.0792	Geraniin	$C_{41} H_{28} O_{27}$	Tannins

6.079	307.081	306.0737	(+)-Gallocatechin	$C_{15}H_{14}O_7$	Flavonoids
6.123	595.1447	594.1367	Kaempferol 3-(5"-feruloylapioside)	$C_{30}H_{26}O_{13}$	Flavonoids
6.463	402.1552	401.1474	Margrapine A	$C_{21}H_{23}NO_7$	Quinolines and derivatives
6.591	652.1166	634.083	Punicacortein A	$C_{27}H_{22}O_{18}$	Tannins
6.641	344.1344	326.1011	Acetylaminodantrolene	$C_{16}H_{14}N_4O_4$	Azolidines
6.754	954.1187	936.0827	Casuarictin	$C_{41}H_{28}O_{26}$	Tannins
6.956	579.1491	578.142	Apigenin 7-(3"-p-coumaroylglucoside)	$C_{30}H_{26}O_{12}$	Flavonoids
7.042	453.104	430.1154	N-Ethylmaleimide-S-glutathione	$C_{16}H_{22}N_4O_8S$	Maleimides
7.042	321.0619	320.0547	2,3-Dihydrogossypetin	$C_{15}H_{12}O_8$	Flavonoids
7.266	386.1601	385.1524	Papaverrubine B	$C_{21}H_{23}NO_6$	Rhoeadine alkaloids
7.327	291.0865	290.0794	Oritin-4beta-ol	$C_{15}H_{14}O_6$	Flavonoids
7.35	471.0187	470.0111	Sanguisorbic acid dilactone	$C_{21}H_{10}O_{13}$	Tannins
7.403	207.1383	206.1309	2-Phenylethyl 3-methylbutanoate	$C_{13}H_{18}O_2$	Fatty Acyls
7.99	437.1077	436.1006	Homomangiferin	$C_{20}H_{20}O_{11}$	Benzopyrans
7.991	305.0664	304.0589	Dihydrorobinetin	$C_{15}H_{12}O_7$	Flavonoids
8.162	479.0828	478.0755	Isoetin 4'-glucuronide	$C_{21}H_{18}O_{13}$	Flavonoids
8.285	465.1019	464.095	5,6,7,3',4'-Pentahydroxy-8-methoxyflavone 7-apioside	$C_{21}H_{20}O_{12}$	Flavonoids
8.285	319.0445	318.0374	Rhodocladonic Acid	$C_{15}H_{10}O_8$	Flavonoids
8.612	491.2857	473.2522	LysoPE(0:0/18:4(6Z,9Z,12Z,15Z))	$C_{23}H_{40}NO_7P$	Glycerophospholipids
8.91	303.0498	302.0425	3,5,7,2',5'-Pentahydroxyflavone	$C_{15}H_{10}O_7$	Flavonoids
9.057	463.0877	462.0799	5,6,7,2'-Tetrahydroxyflavone 7-glucuronide	$C_{21}H_{18}O_{12}$	Flavonoids
9.08	523.2159	522.2092	Isolariciresinol 9-O-beta-D-glucoside	$C_{26}H_{34}O_{11}$	Lignan glycosides
10.168	604.2744	586.2394	Xylocarpus A	$C_{31}H_{38}O_{11}$	Terpenoid
10.514	501.3201	500.3132	Physalolactone B	$C_{30}H_{44}O_6$	Steroids and steroid derivatives
10.515	663.3742	662.3668	1-Acetyl-3,27-dihydroxywitha-5,24-dienolide 3-glucoside	$C_{36}H_{54}O_{11}$	Steroids and steroid derivatives
12.731	228.1958	210.1619	10-Tridecynoic acid	$C_{13}H_{22}O_2$	Fatty Acyls
14.313	460.2703	459.2626	Militarinone A	$C_{26}H_{37}NO_6$	Pyridine alkaloid
14.314	415.212	414.2049	Eplerenone	$C_{24}H_{30}O_6$	Steroids and steroid derivatives
14.653	421.3177	398.3284	Nb-Palmitoyltryptamine	$C_{26}H_{42}N_2O$	Indoles and derivatives

14.973	397.2007	396.193	(S)-(E)-2'-(3,6-Dimethyl-2-heptenyl)-3',4',7-trihydroxyflavanone	$C_{24}H_{28}O_5$	Flavonoids
14.974	281.1384	280.1312	Hymenoflorin	$C_{15}H_{20}O_5$	Prenol lipids
14.974	119.0852	118.078	alpha-Methylstyrene	C_9H_{10}	Terpenoid
14.977	516.2933	515.2872	Candoxatril	$C_{29}H_{41}NO_7$	Indanes
15.195	415.2123	414.2045	Armillarin	$C_{24}H_{30}O_6$	Organooxygen compounds
16.202	353.2697	352.2618	MG(0:0/18:3(6Z,9Z,12Z)/0:0)	$C_{21}H_{36}O_4$	Fatty Acyls
21.143	282.2792	281.2721	Dodemorph	$C_{18}H_{35}NO$	Oxazinanes
22.568	384.3465	383.3394	N-stearoyl valine	$C_{23}H_{45}NO_3$	Fatty Acyls
22.66	338.3422	337.3346	N-Cyclohexanecarbonylpentadecylamine	$C_{22}H_{43}NO$	Fatty Acyls
22.775	593.273	570.2842	Khayanthone	$C_{32}H_{42}O_9$	Prenol lipids
23.184	310.3111	309.3039	N-Hexadecanoylpyrrolidine	$C_{20}H_{39}NO$	Pyrrolidines
25.222	959.5668	936.5796	1,2-Di-(9Z,12Z,15Z-octadecatrienoyl)-3-(Galactosyl-alpha-1-6-Galactosyl-beta-1)-glycerol	$C_{51}H_{84}O_{15}$	Glycerolipids

Green Synthesis of AC-AgNPs

In this study, the optimization of AC-AgNPs synthesis is aimed at achieving the desired size, distribution, and physicochemical properties. According to Kredy (2018), temperature plays a significant role in controlling the reaction rate of nanoparticle formation. The addition of NaOH buffer, making the solution alkaline, enhances the reduction rate during silver nanoparticle formation. Notably, one of the observable indicators of silver nanoparticle formation is the color change of the solution from its initial light green to brown, as previously reported by Bakshi et al. (2015) (Figure 2).

The green synthesis of AC-AgNPs led to distinct color changes at temperatures of 60°C, 70°C, and 80°C. The solution's initial light green color gradually transformed to transparent yellow and eventually to brown as the synthesis proceeded. At each temperature, the formation of AC-AgNPs, as indicated by the brown color change, became visible at different time points. Notably, at 70°C and 80°C, the brown turbidity appeared earlier than at 60°C, showcasing the influence of temperature on the synthesis kinetics. Moreover, the introduction of NaOH not only affected the color but also raised the solution's pH from acidic to alkaline, indicating its role in the synthesis process.

After completing the nanoparticle synthesis, high-speed centrifugation was employed to precipitate the silver nanoparticles. The collected particles were then dried to obtain solid nanoparticles, with the corresponding yields recorded in Table 2. The results highlight that increasing the pH to an alkaline level and elevating the temperature generally led to higher yields. These findings align with Kredy's (2018) observations and indicate that optimizing pH and temperature can facilitate efficient redox reactions and enhance particle growth. The pH influences the stability and rate of silver nanoparticle formation, while temperature affects the reaction rate and overall yield.

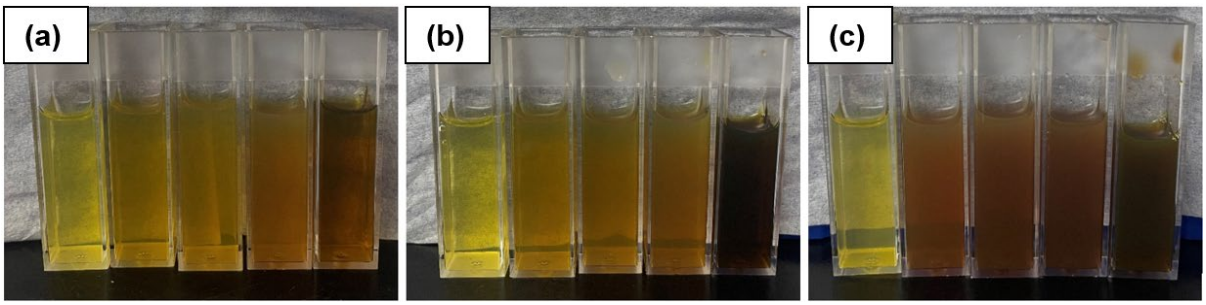

Figure 2: Results of Nanoparticle Synthesis (a) 60ºC, (b) 70ºC, and (c) 80ºC

Table 2: Results of optimization of synthesis temperature and pH on the yield of AC-AgNPs

Optimization conditions		Parameters
Temperature (ºC)	**pH**	**Dry yield (mg)**
60	4	7
	9	12
70	4	10
	9	9
80	4	6
	9	12

Characterization of AC-AgNPs

UV-Vis Spectrophotometer Analysis

The UV-Vis spectrophotometer analysis (Figure 3) reveals that absorbance increased over time at 60°C and 70°C, indicating a direct relationship between synthesis duration and the reduction rate. According to Oktaviani and Amrullah (2009), absorbance in the range of 400–450 nm is typically associated with silver nanoparticles (Ag^0), while silver ions (Ag^+) are linked with absorbance in the 370-400 nm range. The addition of NaOH at 60°C and 70°C resulted in a shift of the peak wavelength to 424 nm and 412 nm, confirming the formation of pure silver AgNPs. Lower temperatures led to larger nanoparticles with longer wavelengths, while higher temperatures yielded smaller nanoparticles. AgNPs did not form at 80°C, likely due to unsuitable conditions. This underscores the critical role of temperature and reaction time in silver nanoparticle synthesis (Ibrahim, 2015; Patra and Baek, 2014).

Particle Size and Zeta Potential Analysis

Particle size and size distribution analysis, performed with a Particle Size Analyzer (PSA) at temperatures of 60°C and 70°C and under varying pH conditions (4 and 9), revealed significant insights. The average particle size exhibited a direct relationship with pH alterations at both temperatures. At pH 4, the particle sizes were approximately 518.8 nm (60°C) and 502.6 nm (70°C). In contrast, at pH 9, the particle sizes decreased to 147.1 nm (60°C) and 135.5 nm (70°C). The smallest particles were achieved at a pH of 9 and a synthesis temperature of 70°C. This is in line with previous studies suggesting that higher pH leads to a faster reaction rate and smaller particle size (Marciniak et al., 2020). The accepted descriptive range for nanoparticle size is between 1-100 nm, as supported by numerous studies (Susanti et al., 2022). In the pharmaceutical field, nanoparticles are also defined as particles with diameters ranging from 10-1000 nm (Mazayen et al., 2022).

Zeta potential analysis, a crucial indicator of stability, revealed values of -40.4±8.79 mV (60°C) and -45.1±11.7 mV (70°C) after the addition of NaOH (Table 3). Zeta potential values exceeding +30 mV or falling below -30 mV indicate stability, with values within this range being unstable and prone to aggregation. The results demonstrate the stable conditions of AC-AgNPs, emphasizing their potential for cellular uptake and long-term structural integrity (Lin et al., 2014).

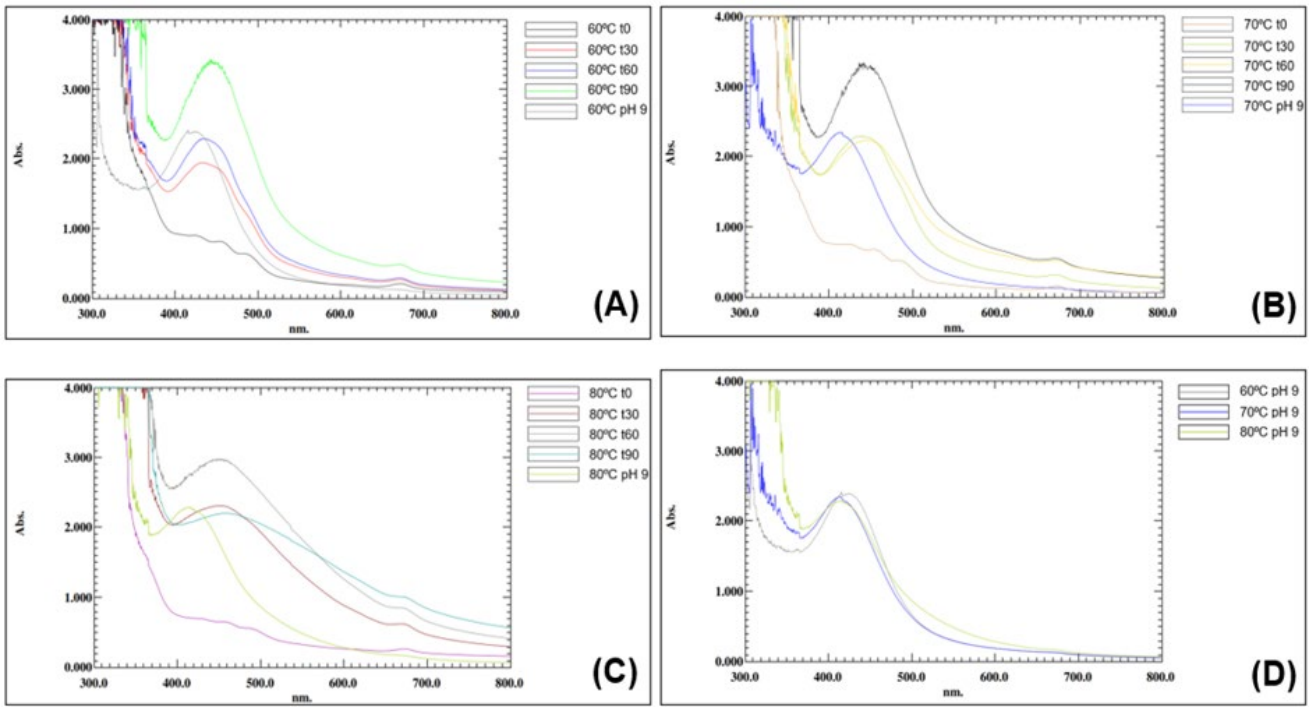

Figure 3: Comparison of solution absorbance at each temperature with time (A) 60ºC; (B) 70ºC; (C) 80ºC and (D) addition of NaOH

Table 3: Particle size and zeta potential of AC-AgNPs

Particle size analysis		
Temperature (ºC)	**pH**	**Z-Average (d.nm)**
60	4	518.8
	9	147.1
70	4	502.6
	9	135.5
Zeta potential analysis		
Temperature (ºC)	**pH**	**Zeta potential (mV)**
60	9	-40.4±8.79
70	9	Nd

Nd: not determined.

FTIR Analysis

The FTIR spectra of the synthesized silver nanoparticles (AC-AgNPs) are presented in Figure 4, revealing absorption peaks that confirm the presence of various functional groups within the plant extract involved in silver nanoparticle formation. The peak at 3363.42 cm^{-1} indicates the presence of hydrogen bonds (O-H) from alcohol compounds. Peaks at 2922.28 cm^{-1} and 2852.16 cm^{-1} signify (C-H) stretching, related to alkene groups. The absorption band at 1729.37 cm^{-1} represents carbonyl compounds like ketones, aldehydes, esters, or carboxyls, while the peak at 1607.9 cm^{-1} indicates double bonds or aromatic compounds with (C=C) stretching. The absorption bands at 1454.94 cm^{-1} and 1375.81 cm^{-1} confirm the presence of methyl compounds through bending vibrations (C-H). Furthermore, primary and secondary amine compounds with stretching (C-N) are validated by absorption bands at 1159.14 cm^{-1} and 1032.58 cm^{-1}. Previous research by Abdi et al. (2012) and Sankar and Abideen (2015) also employed FTIR to identify these functional groups, which have the ability to reduce AgNPs (Gnanadesigan et al., 2011).

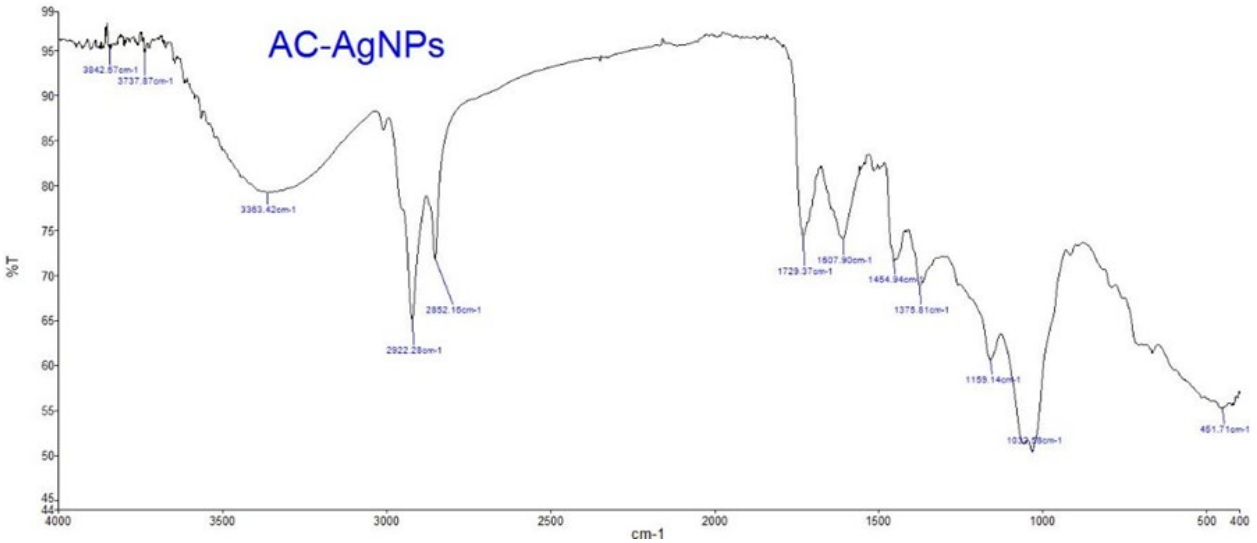

Figure 4: FTIR spectrum of AC-AgNPs

SEM Analysis

The morphology of the synthesized silver nanoparticles was characterized using Scanning Electron Microscopy (SEM) presents the observation results, indicating that silver nanoparticles produced with *A. corneri* leaf extract at 70°C and pH 9 exhibit a spherical shape. This spherical shape is typical of silver nanoparticles as they tend to form structures with the minimum surface area, which is the most thermodynamically stable configuration. The particle's growth kinetics during synthesis play a role in shaping these nanoparticles (Sau and Rogach, 2010).

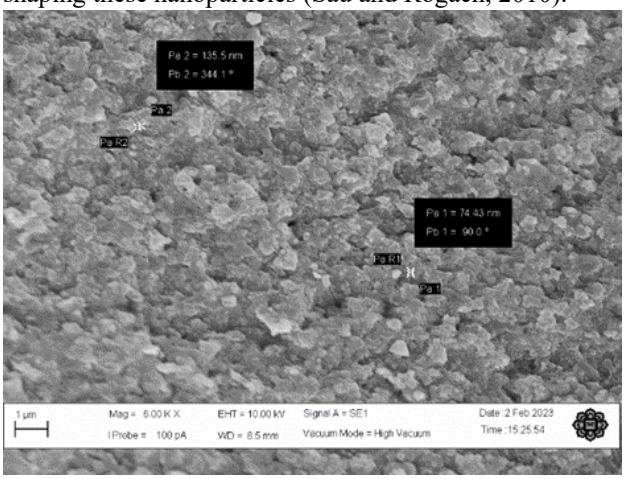

Figure 5: Morphology of AC-AgNPs Using SEM at Observation with a Magnification of 4.00 KX

Antimicrobial Activity of AC-AgNPs

The results of inhibitory zone measurements in the antimicrobial activity test are presented in Figure 6 and Table 4. The antimicrobial activity results revealed the effectiveness of the synthesized AC-AgNPs against various bacteria, emphasizing their inhibitory zones in comparison to control groups and $AgNO_3$. Testing the AC-AgNPs synthesized at 70°C with NaOH revealed inhibitory zones against all tested bacteria, with average inhibition diameters ranging from 8.33 to 10.00 mm.

Notably, these AC-AgNPs showed larger inhibition zones than the $AgNO_3$ solution, indicating the enhanced antibacterial efficacy of AC-AgNPs due to their smaller size, increased surface area, and more effective interaction with microorganisms. In contrast, *A. corneri* leaf extract and the negative control (DMSO 10%) exhibited no antimicrobial activity. The antimicrobial activity of AC-AgNPs was particularly potent against Gram-positive bacteria, with the largest inhibition observed against *S. aureus*.

This pattern aligns with previous studies, attributing the increased effectiveness against Gram-positive bacteria to differences in cell wall structure and membrane composition. While Gram-positive bacteria have peptidoglycan-rich thick cell walls that are sensitive to silver nanoparticles, Gram-negative bacteria's outer membrane structure, often fortified with lipopolysaccharides serves as a protective barrier, reducing the penetration of silver nanoparticles (Tang et al., 2013; Siddiqui et al., 2019).

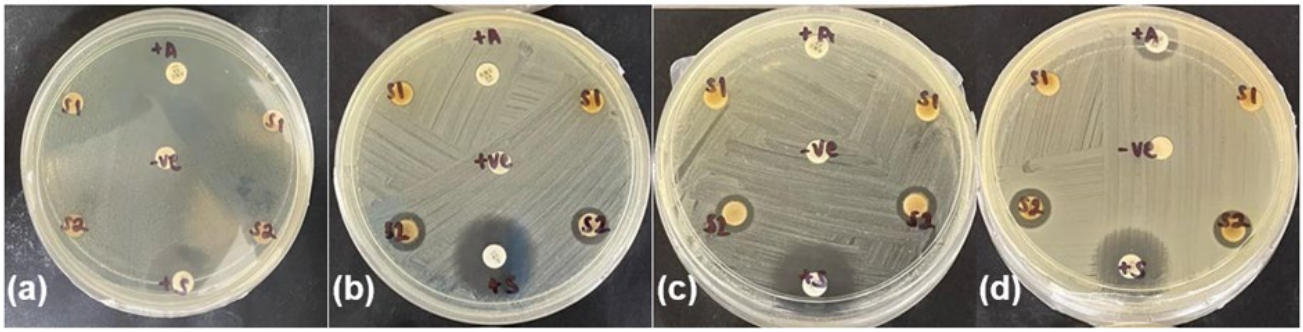

Figure 6: Antimicrobial activity of AC-AgNPs is indicated by +S on (a) *P. aeruginosa*, (b) *E. coli*, (c) *B. subtilis*, and (d) *S. aureus*

Table 4: Results of Inhibitory Zone Measurements in Antimicrobial Activity Testing

No.	Test Sample	Inhibition Zone (mm)			Average (mm)
		1	2	3	
Bacteria: *Pseudomonas aeruginosa*					
1.	Positive control (Streptomycin)	21	24	25	23.33
2.	Negative control (DMSO 10%)	0	0	0	0.00
3.	*A. corneri* leaf extract	0	0	0	0.00
4.	10 mM $AgNO_3$ solution	9	8	8	8.33
5.	AgNPs	7	9	9	8.33
Bacteria: *Escherichia coli*					
1.	Positive control (Amoxicillin)	7	0	0	2.33
2.	Positive control (Streptomycin)	24	24	15	21.00
3.	Negative control (DMSO 10%)	0	0	0	0.00
4.	*A. corneri* leaf extract	0	0	0	0.00
5.	10 mM $AgNO_3$ solution	9	9	8	8.67
6.	AgNPs	9.5	10	7	8.83
Bacteria: *Bacillus subtilis*					
1.	Positive control (Amoxicillin)	7	0	0	2.33
2.	Positive control (Streptomycin)	25	15	22	20.67
3.	Negative control (DMSO 10%)	0	0	0	0.00
4.	*A. corneri* leaf extract	0	0	0	0.00
5.	10 mM $AgNO_3$ solution	9	9	9	9.00
6.	AgNPs	10	7	11	9.33
Bacteria: *Staphylococcus aureus*					
1.	Positive control (Amoxicillin)	9	12	8	9.67
2.	Positive control (Streptomycin)	23	20	11	18.00
3.	Negative control (DMSO 10%)	0	0	0	0.00
4.	*A. corneri* leaf extract	0	0	0	0.00
5.	10 mM $AgNO_3$ solution	8	8	8	8.00
6.	AgNPs	11.5	10.5	8	10.00

Cytotoxic Activity of AC-AgNPs

The MTT assay was employed to evaluate the cytotoxicity of AC-AgNPs on MCF-7 breast cancer cells, revealing a dose-dependent reduction in cell viability. The IC_{50} value was determined to be 74.9 µg/mL, classifying AC-AgNPs' cytotoxic activity as moderate according to the US National Cancer Institute (NCI), as shown in Figure 7. This research underlines the potential of AC-AgNPs as a cytotoxic agent.

MCF-7 cells were chosen for their extensive use in cytotoxicity research and the reliability of results due to their genetic stability. Furthermore, the study draws upon previous literature supporting silver nanoparticles' effectiveness in cytotoxic assays against MCF-7 cells, showcasing their potential for cancer treatment (Ali et al., 2021; Firdhouse and Lalitha, 2015).

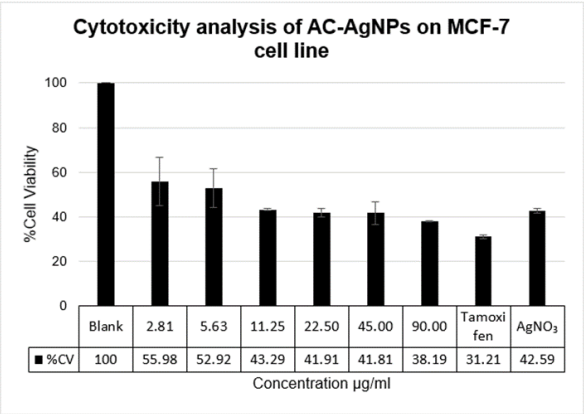

Figure 7: Cytotoxic Activity of AC-AgNPs Assessed by MTT Method

Conclusion

Green synthesis of silver nanoparticles using *A. corneri* leaf extract at a temperature of 70°C and pH 9 has successfully yielded spherical silver nanoparticles with a particle size of 135.5 nm and a zeta potential value of -45.1±11.7 mV. These nanoparticles have exhibited antimicrobial activity against both Gram-negative and Gram-positive bacteria, including *P. aeruginosa*, *E. coli* for Gram-negative bacteria, and *B. subtilis*, *S. aureus* for Gram-positive bacteria, falling within the moderate category. Furthermore, the silver nanoparticles have demonstrated cytotoxic activity against MCF-7 breast cancer cell lines, with an IC_{50} value of 74.9 µg/ml, also categorized as moderate. This research not only presents a green and eco-friendly method for synthesizing silver nanoparticles but also showcases their potential applications in combating bacterial infections and cancer treatment. The findings contribute to the advancement of nanotechnology and offer new possibilities in addressing critical health challenges.

Authors Contributions

Conceptualization, M.T.; methodology, M.T., D.S., and I.R.; conduct the research and collect the data, I.R.; writing—original draft preparation, I.R.; writing—review and editing, M.T., and M.N.; supervision, M.N., M.T., and D.S.; project administration, M.N., M.T., and D.S.; funding acquisition, M.T., and D.S. All authors have read and agreed to the published version of the manuscript.

Acknowledgement

The authors wish to thank the International Islamic University Malaysia, Kuantan, Malaysia, for the facilitating mobility programme for I.R.

Conflict of Interest

The authors declare that there is no conflict of interest in the writing of this manuscript.

References

Abdi, V., Sourinejad, I., Yousefzadi, M., & Ghasemi, Z. (2018). Mangrove-mediated synthesis of silver nanoparticles using native Avicennia marina plant extract from southern Iran. *Chemical Engineering Communications, 205*(8), 1069-1076. https://doi.org/10.1080/00986445.2018.1431624

Ali, A., Banerjee, S., Kamaal, S., Us-man, M., Das, N., Afzal, M., Alarifi, A., Sepay, N., Roy, P., Ahmad, M. (2021). Ligand substituent effect on the cytotoxicity activity of two new copper(ii) complexes bearing 8-hydroxyquinoline derivatives: validated by MTT assay and apoptosis in MCF-7 cancer cell line (human breast cancer). *RSC Adv. 11*(24), 14362-14373. doi: 10.1039/d1ra00172h.

Bari, N. A. A., Ferdosh, S., & Sarker, M. Z. I. (2021). Antimicrobial and Antioxidant Activities of A Malaysian Medical Plant Anisophyllea disticha (Jack) Baill. and Quantification of Its Phenolic Constituents. *Bangladesh J. Bot, 50*(3), 515-521. https://doi.org/10.3329/bjb.v50i3.55830

Bakshi, M., Ghosh, S., & Chaudhuri, P. (2015). Green synthesis, characterization and antimicrobial potential of silver nanoparticles using three mangrove plants from Indian Sundarban. *BioNanoScience, 5*, 162-170. https://doi.org/10.1007/s12668-015-0175-8

Böhmert, L., Niemann, B., Thüne-mann, A. F., & Lampen, A. (2012). Cytotoxicity of peptide-coated silver nanoparticles on the human intestinal cell line Caco-2. *Archives of toxicology, 86*(7), 1107-1115. https://doi.org/10.1007/s00204-012-0840-4

Eze, F. N., Tola, A. J., Nwabor, O. F., & Jayeoye, T. J. (2019). Centella asiatica phenolic extract-mediated bio-fabrication of silver nanoparticles: Characterization, reduction of industrially relevant dyes in water and antimicrobial activities against foodborne pathogens. *RSC Advances, 9*(65), 37957–37970. https://doi.org/10.1039/c9ra08618h

Firdhouse, J., & Lalitha, P. (2015). Apoptotic efficacy of biogenic silver nanoparticles on human breast cancer MCF-7 cell lines. *Progress in biomaterials, 4*, 113. https://doi.org/10.1007/s40204-015-0042-2

Gnanadesigan, M., Anand, M., Ra-vikumar, S., Maruthupandy, M., Ali, M. S., Vijayakumar, V., & Kumaraguru, A. K. (2011). Anti-bacterial potential of biosynthesised silver nanoparticles using Avicennia marina mangrove plant. *Appl Nanosci, 2*, 143-147. https://doi.org/10.1007/s13204-011-0048-6

Ibrahim, H. (2015). Green synthesis and characterization of silver nanoparticles using banana peel extract and their antimicrobial activity against representative microorganisms. *J. Rad Res App Sci, 8*(3), 265-275. https://doi.org/10.1016/j.jrras.2015.01.007

Kredy, H. M. (2018). The effect of pH, temperature on the green synthesis and biochemical activities of silver nanoparticles from Lawsonia inermis extract. *Journal of Pharmaceutical Sciences and Research, 10*(8), 2022-2026.

Lin, P. C., Lin, S., Wang, P. C., & Srdhar, R. (2014). Techniques for physicochemical characterization of nanomaterials. *Biotechnology advances, 32*(4), 711-726. https://doi.org/10.1016/j.biotechadv.2013.11.006

Loo, Y. Y., Rukayadi, Y., Nor-Khaizura, M.-A.-R., Kuan, C. H., Chieng, B. W., Nishibuchi, M., & Radu, S. (2018). In Vitro Antimicrobial Activity of Green Synthesized Silver Nanoparticles Against Selected Gram-negative Foodborne Pathogens. *Frontiers in Microbiology, 9*. https://doi.org/10.3389/fmicb.2018.01555

Marciniak, L., Nowak, M., Trojanowska, A., Tylkowski, B., & Jastrzab, R. (2020). The Effect of pH on the Size of Silver Nanoparticles Obtained in the Reduction Reaction with Citric and Malic Acids. *Materials (Basel), 13*(23), 5444. https://doi.org/10.3390/ma13235444

Mazayen, Z. M., Ghoneim, A. M., Elbatanony, R. S., Basalious, E. B., & Bendas, E. R. (2022). Pharmaceutical nanotechnology: from the bench to the market. *Future Journal of Pharmaceutical Sciences, 8*(1). https://doi.org/10.1186/s43094- 022-00400-0

Mustapha, T., Misni, N., Ithnin, N. R., Daskum, A. M., & Unyah, N. Z. (2022). A Review on Plants and Microorganisms Mediated Synthesis of Silver Nanoparticles, Role of Plants Metabolites and Applications. *Int. J. Environ. Res. Public Health, 19*(2), 674. https://doi.org/10.3390/ijerph19020674

O'Bryan, C. A., Crandall, P. G., & Ricke, S. C. (2018). Antimicrobial resistance in foodborne pathogens. *In Food and feed safety systems and analysis*, 99-115. Academic Press. https://doi.org/10.1016/B978-0-12-811835-1.00006-3

Oktaviani, D. T., F, D. C., & Amrullah, A. (2015). Sintesis Nano Ag dengan Metode Reduksi Kimia. *Sainteknol: Jurnal Sains dan Teknologi, 13*(2). https://doi.org/10.15294/sainteknol.v13i2.5242

Onivogui, G., Letsididi, R., Diaby, M., Wang, L., & Song, Y. (2016). Influence of extraction solvents on antioxidant and antimicrobial activities of the pulp and seed of Anisophyllea laurina R. Br. ex Sabine fruits. *Asian Pac J Trop Biomed, 6*(1), 20–25. http://dx.doi.org/10.1016/j.apjtb.2015.09.023

Patel, L. N., Uchiyama, T., Kim, K. J., Borok, Z., Crandall, E. D., Shen, W. C., & Lee, V. H. (2008). Molecular and functional expression of multidrug resistance-associated protein-1 in primary cultured rat alveolar epithelial cells. *Journal of pharmaceutical sciences, 97*(6), 2340-2349. https://doi.org/10.1002/jps.21134

Patil, M. P., & Kim, G. D. (2017). Eco-friendly approach for nanoparticles synthesis and mechanism behind antibacterial activity of silver and anticancer ativity of gold nanoparticles. *Applied microbiology and biotechnology, 101*(1), 79-92. https://doi.org/10.1007/s00253-016-8012-8

Patra, J. K., & Baek, K. H. (2014). Green nanobiotechnology: factors affecting synthesis and characterization techniques. *Journal of Nanomaterials, 219*. https://doi.org/10.1155/2014/417305

Sankar, M. V., & Abideen, S. (2015). Pesticidal effect of Green synthesized silver and lead nanoparticles using Avicennia marina against grain storage pest Sitophilus oryzae. *International Journal of Nanomaterials and Biostructures, 5*(3), 32-39.

Sau, T. K., & Rogach, A. L. (2010). Nonspherical Noble Metal Nanoparticles: Colloid-Chemical Synthesis and Morphology Control. *Advanced Materials, 22*(16), 1781-1804. doi:10.1002/adma.200901271

Shembele, B., Mahlangeni, N., & Moodley, R. (2022). Biosynthesis and bioactivities of metal nanoparticles mediated by Helichrysum aureonitens. *Journal of Analytical Science and Technology, 13*(8), 1-11. https://doi.org/10.1186/s40543-022-00316-7

Siddiqui, M. T., Mondal, A. H., Sultan, I., A, A., & M. R., H. Q. (2019). Co-occurrence of ESBLs and silver resistance determinants among bacterial isolates inhabiting polluted stretch of river Yamuna, India. *International Journal of Environmental Science and Technology, 16*, 5611–5622. https://doi.org/10.1007/s13762-018-1939-9

Suriyakala, G., Sathiyaraj, S., Babujanarthanam, R., Alarjani, K. M., Hussein, D. S., Rasheed, R. A., & Kanimozhi, K. (2022). Green synthesis of gold nanoparticles using Jatropha integerrima Jacq. flower extract and their antibacterial activity. *Journal of King Saud University - Science, 34*(3). https://doi.org/10.1016/j.jksus.2022.101830

Susanti, D., Haris, M. S., Taher, M., & Khotib, J. (2022). Natural Products-Based Metallic Nanoparticles as Antimicrobial Agents. *Frontiers in Pharmacology, 13*. Frontiers Media S.A. https://doi.org/10.3389/fphar.2022.895616

Tang, J., Chen, Q., Xu, L., Zhang, S., Feng, L., Cheng, L., Xu, H., Liu, Z., & Peng, R. (2013). Graphene Oxide–Silver Nanocomposite as a Highly Effective Antibacterial Agent with Species-Specific Mechanisms. *ACS Applied Materials & Interfaces, 5*(9), 3867–3874. https://doi.org/10.1021/am4005495

Tanwar, J., Das, S., Fatima, Z., & Hameed, S. (2014). Multidrug resistance: an emerging crisis. *Interdisciplinary perspectives on infectious diseases, 2014*. https://doi.org/10.1155/2014/541340

WHO (2023). Antimicrobial resistance. Retrieved from: https://www.who.int/news-room/fact-sheets/detail/antimicrobial-resistance, 30 January 2024

Zhang, X, F., Liu, Z. G., Shen, W., & Gurunathan, S. (2016). Silver Nanoparticles: Synthesis, Characterization, Properties, Applications, and Therapeutic Approaches. *Int J Mol Sci, 17*(9), 1534. https://doi.org/10.3390/ijms17091534

Zuhrotun, A., Oktaviani, D. J., & Hasanah, A. N. (2023). Biosynthesis of Gold and Silver Nanoparticles Using Phytochemical Compounds. *Molecules, 28*(7), 3240. https://doi.org/10.3390/molecules28073240